Resolving the transition from negative to positive blood oxygen level-dependent responses in the developing brain

Mariel G. Kozberg[1], Brenda R. Chen, Sarah E. DeLeo, Matthew B. Bouchard, and Elizabeth M. C. Hillman[1]

Laboratory for Functional Optical Imaging, Departments of Biomedical Engineering and Radiology, Columbia University, New York, NY 10027

The adult brain exhibits a local increase in cortical blood flow in response to external stimulus. However, broadly varying hemodynamic responses in the brains of newborn and young infants have been reported. Particular controversy exists over whether the "true" neonatal response to stimulation consists of a decrease or an increase in local deoxyhemoglobin, corresponding to a positive (adult-like) or negative blood oxygen level-dependent (BOLD) signal in functional magnetic resonance imaging (fMRI), respectively. A major difficulty with previous studies has been the variability in human subjects and measurement paradigms. Here, we present a systematic study in neonatal rats that charts the evolution of the cortical blood flow response during postnatal development using exposed-cortex multispectral optical imaging. We demonstrate that postnatal-day-12–13 rats (equivalent to human newborns) exhibit an "inverted" hemodynamic response (increasing deoxyhemoglobin, negative BOLD) with early signs of oxygen consumption followed by delayed, active constriction of pial arteries. We observed that the hemodynamic response then matures via development of an initial hyperemic (positive BOLD) phase that eventually masks oxygen consumption and balances vasoconstriction toward adulthood. We also observed that neonatal responses are particularly susceptible to stimulus-evoked systemic blood pressure increases, leading to cortical hyperemia that resembles adult positive BOLD responses. We propose that this confound may account for much of the variability in prior studies of neonatal cortical hemodynamics. Our results suggest that functional magnetic resonance imaging studies of infant and child development may be profoundly influenced by the maturing neurovascular and autoregulatory systems of the neonatal brain.

neurovascular coupling | brain development | autoregulation | vascular compartments | somatosensory stimulation

In the adult brain, sensory stimulation leads to an increase in cerebral blood flow in a particular region of the corresponding sensory cortex. Although it has been shown that increased oxygen consumption occurs in the activated region because of increased neuronal activity, the adult blood flow response increases delivery of oxygenated blood to the activated region and, in most cases, this blood flow increase outstrips oxygen consumption. The result is an overall increase in local oxygenation and blood volume, leading to a local increase in oxygenated hemoglobin (HbO) and total hemoglobin (HbT) and a decrease in deoxygenated hemoglobin (HbR) concentrations (1–3). The functional magnetic resonance imaging (fMRI) blood oxygen level-dependent (BOLD) signal is sensitive to changes in the concentration of paramagnetic HbR (1). A normal "positive BOLD" response would therefore correspond to a decrease in local HbR, whereas a "negative BOLD" response would correspond to an increase in local HbR.

Despite the hemodynamic response being relatively well defined in adults, it is not fully understood throughout development. Prior studies of the neonatal hemodynamic response to stimuli have yielded widely conflicting results (4–19). fMRI studies generally only examine changes in HbR via BOLD, whereas near infrared spectroscopy (NIRS) is a noninvasive optical technique

capable of discerning HbO, HbR, and HbT changes. Studies using both fMRI and NIRS have reported dramatically different responses that fall into two general categories: (*i*) a positive response (a decrease in local HbR) resembling adult functional hyperemia using fMRI (9, 10) and NIRS (5, 11) and (*ii*) an inverted response (an increase in local HbR), using fMRI (7, 8, 12–14, 16–19) and NIRS (4, 15). This lack of consistency has been difficult to reconcile, because many of these studies focused on human neonatal populations, did not follow the same subjects throughout development, were limited in subject numbers, used various different stimulation paradigms, and had additional confounds such as depth of sedation and level of attention. Additionally, many studies were conducted in premature infants or infants with other medical conditions, whose health may have been a confound. Therefore, despite several studies seeking to determine the "ground truth" regarding neonatal functional hyperemia (9, 11), confusion remains about the nature, cause, and interpretability of stimulus-induced hemodynamic changes in the developing brain. Reconciling these observations is of prime importance to the growing field of neonatal and developmental fMRI research (6, 20) and could also lead to an improved understanding of neonatal brain development and, thus, the diagnosis, treatment, and management of neonatal neurological conditions.

The purpose of this study was to systematically explore the properties of the hemodynamic response to stimulus in the developing rat brain. Specifically, we sought to address whether hemodynamic response inversion was routinely seen, and if so, how it manifested at the level of single vessels and resolved with the progression toward adulthood. Data were acquired by using multispectral optical intrinsic signal imaging (MS-OISI) of the cortex through a thinned-skull, or skull-removed, craniotomy to capture the hemodynamic response to somatosensory stimulation in neonatal rat pups of gradually increasing age. MS-OISI data represents a superficially weighted sum of signals from the cortex, penetrating deep enough to detect changes in capillary beds (21) and having sufficient resolution to map changing HbO and HbR concentrations in pial vessels, and allowing calculation of changes in their diameter. Changes in HbT correspond to changes in the tissue concentration of red blood cells, which in turn suggest changes in vascular resistance and therefore blood flow. This high-speed imaging approach enabled spatially resolved examination of vascular and oximetric cortical responses to hindpaw stimulation at a range of postnatal ages (22, 23).

www.manaraa.com

Results

Animals were prepared and imaged as described in *Methods*. Resulting data consisted of movies of changes in HbR, HbO, and HbT at 25 frames per second in response to a 4-s hindpaw somatosensory stimulation (24). In a subset of experiments, intra-arterial blood pressure was simultaneously measured during image acquisition. Data were analyzed to generate difference images showing regional responses to stimulation, and time-courses were extracted from selected regions of the images.

Blood Pressure Confounds. An important initial finding in our studies was the effect of stimulus-evoked systemic blood pressure fluctuations on cortical hemodynamics in the neonatal brain, which we hypothesized could account for some of the paradoxical findings in prior studies of the neonatal hemodynamic response. We performed a set of experiments in which intraarterial blood pressure was continually monitored during imaging via cannulation of the femoral artery. Stimulus amplitude was varied systematically. In postnatal-day-12–13 (P12–P13) pups, assumed to be equivalent in relative age to human newborns (21), we found that at higher stimulus amplitudes, a systemic blood pressure increase was observed, and that this response directly translated into an increase in cortical HbT, as shown in Fig. 1 *A* and *B*. The resulting "cortical blood pressure response" (Fig. 1*C*; generated from runs in which a systemic blood pressure increase was observed) closely resembles the positive adult hemodynamic response, with an increase in HbO and HbT and a decrease in HbR (positive BOLD). However, when no blood pressure increase is observed, the cortical response is inverted and prolonged, with an increase in HbR, a decrease in HbO, and a delayed decrease in HbT (negative BOLD; Fig. 1*D*). Fig. S1 *A* and *B* shows that in the neonatal brain the magnitude of the cortical HbT response to stimulus is linearly correlated to the magnitude of systemic blood pressure response. Using the same range of stimulus intensities in adult rats resulted in blood pressure increases only in the highest stimulus intensity range (2 mA +), while cortical responses resembled "normal" positive adult responses, irrespective of stimulus

intensity (Fig. S2). The magnitude of the systemic blood pressure response in adults was not correlated to the magnitude of the cortical HbT response (Fig. S1 *C* and *D*). These observations are consistent with the presence of immature cerebral autoregulation in the neonatal brain, allowing systemic blood pressure changes to directly impact cortical blood flow.

Fig. 1 also shows a decrease in systemic blood pressure in response to low-amplitude stimuli in neonates. A blood pressure decrease is also observed in adults (Fig. S2*A*), suggesting that this effect is not specific to neonates. Previous studies have indicated that this effect occurs via a supraspinal control mechanism suppressing catecholamine release from the adrenal glands (25–27). We note that the correlation between negative HbT and blood pressure changes in neonates is not as strong as within the positive range (Fig. S1 *A* and *B*), but poor autoregulation could potentially allow these negative changes in blood pressure to influence cortical blood flow, as discussed further below. Importantly, when blood pressure decreases occur in the adult, cortical HbT responses remain positive (Figs. S1 *C* and *D* and S2).
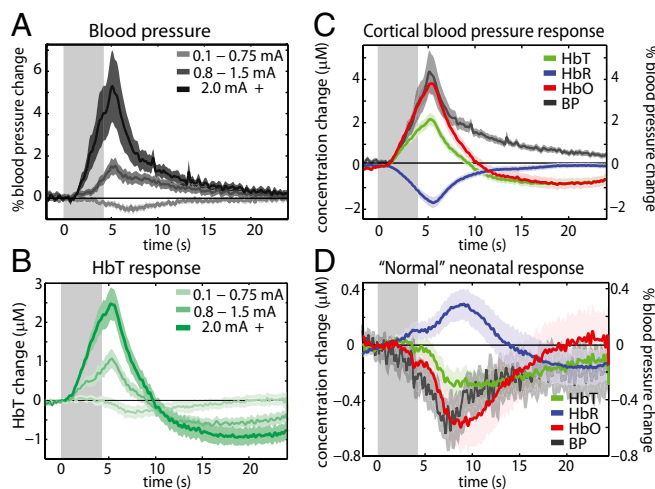
Evolution of the Hemodynamic Response with Increasing Age. Using sufficiently low stimulus amplitudes (generally less than 0.8 mA) to avoid blood pressure increases, data were then acquired within three age groups (P12–P13, P15–P18, and adult P80+) and analyzed to extract HbO, HbR, and HbT time-courses from the hindpaw region of the somatosensory cortex.

A clearly defined pattern from inversion to the adult positive response can be seen in Fig. 2 *A–C* and *F*. In P12–P13 animals, the response to 4-s hindpaw stimulation consisted of a decrease in HbO and an increase in HbR with a delayed decrease in HbT (negative BOLD; Fig. 2*A*). On average, a brief initial increase in HbT was observed (Fig. 2*E*), although in some animals this early peak was not seen at all. We observe that HbO decreases and HbR increases before the decrease in HbT, such that HbT peaks after HbO ($P < 0.05$) (Fig. 2*D*) and crosses a line $2.5e{-}7$ M below baseline after HbO ($P < 0.01$). We interpret this pattern as evidence of increased oxygen consumption. This phase is then followed by a decrease in HbT, suggesting a blood flow decrease and, thus, an increase in blood transit time resulting in a continuing decrease in HbO and increase in HbR.

The P15–P18 time-courses (Fig. 2*B*) reveal an initial, small positive response (increase in HbO and HbT), followed by a large "undershoot" in which HbO and HbT decrease below baseline, and HbR increases. The early HbT increase is significantly larger ($P < 0.01$) than in P12–P13 rats (Fig. 2*E*). HbO levels cross a line $2.5e{-}7$ M below baseline before HbT ($P < 0.01$), suggesting that the initial hyperemia is unable to fully meet oxygen consumption demands. As in the younger age group, the delayed decrease in HbT causes a prolonged increase in HbR.
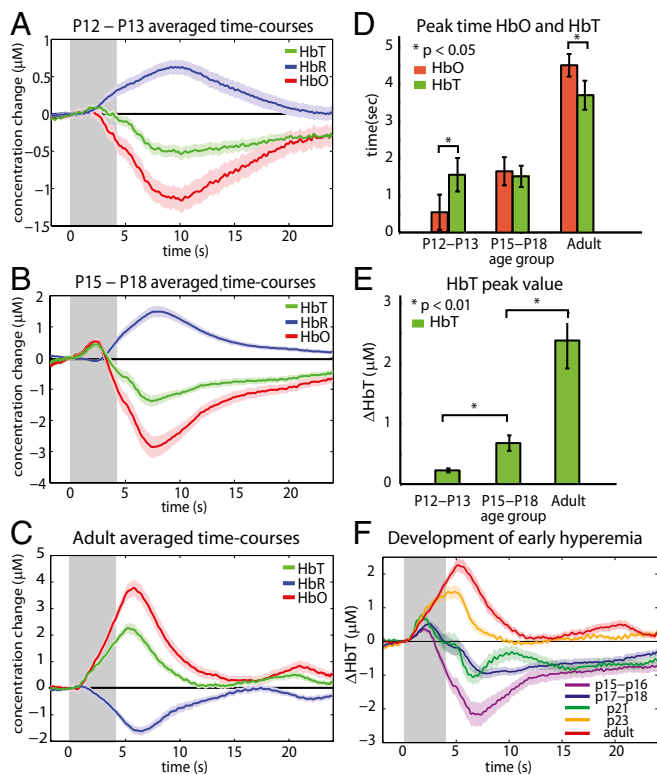
Adult time-courses resemble a classic response dominated by a large increase in HbT and HbO with a corresponding decrease in HbR (positive BOLD; Fig. 2*C*). This response shows a strong and rapid overperfusion of the responding region, exceeding oxygen consumption, with an HbT increase that is significantly larger than the early increase in the P15–P18 age group ($P < 0.01$) (Fig. 2*E*). Fig. 2*F* shows cortical HbT responses from a series of rats imaged between the ages of P15 and P23. As anticipated from Fig. 2 *A–C*, a gradual evolution of increasing initial hyperemia with increasing age can be observed. The response becomes wholly positive by around P23.

Neonatal Negative BOLD. The nature and cause of the inverted, negative BOLD response in neonatal populations has long been debated (12, 18). Our results suggest that almost no increase in blood delivery occurs in response to stimulus in the P12–P13 neonatal age group, which one might expect to result in local deoxygenation and negative BOLD due to oxygen consumption alone. However, we also observe a distinct decrease in HbT in

Fig. 1. Blood pressure effects on the neonatal hemodynamic response. (*A*) Systemic blood pressure recordings from a femoral arterial line in P12–P13 rats undergoing 4-s, 3-Hz hindpaw stimulation of different amplitudes (*n* = 7 rats, averaging 33, 30, and 26 runs for low-to-high stimulus amplitudes, respectively). (*B*) Cortical HbT responses recorded in the same groups as in *A*. Average P12–P13 cortical hemodynamic response from runs in which systemic blood pressure increases were observed (*C*) (*n* = 7 rats, 43 runs), and average P12–P13 cortical hemodynamic response from runs in which systemic blood pressure increases were not observed (*D*) (*n* = 7 rats, 46 runs), both overlaid with corresponding average systemic blood pressure response.

Kozberg et al.

NEUROSCIENCE

www.manaraa.com

Fig. 2. Progression from an inverted neonatal response to an adult response. Time-courses were generated by averaging HbO, HbR, and HbT traces from responding regions across rats in each age group (A) An inverted and prolonged response is observed in P12–P13 age group (*n* = 13 rats, runs = 72). (B) Intermediate age group of P15–P18 shows a small adult-like positive response, followed by a large undershoot (*n* = 9 rats, runs = 68). (C) Classic adult hemodynamic response in P80+ rats (*n* = 8 rats, runs = 67). (D) HbO peaks before HbT in younger animals ($P < 0.05$) and after HbT in older animals ($P < 0.05$). (E) The initial peak HbT response amplitude increases significantly with age ($P < 0.01$). (F) Averaged time-courses for five different age ranges (*n* = 4, 5, 2, 2, 9 rats and runs = 25, 43, 27, 22, 67, respectively). Note: *A–C*, and *F* show mean ± SEMs and time-courses averaged across all runs in each age group. Averages shown in *D* and *E* were calculated by first averaging all runs within an animal, and then using these single rat averages to calculate parameters and to generate age group averages and SEMs.

response to stimulation, exacerbating poststimulus deoxygenation. Experiments with bilateral exposures of the somatosensory cortex were performed to further explore these components in the neonatal brain.
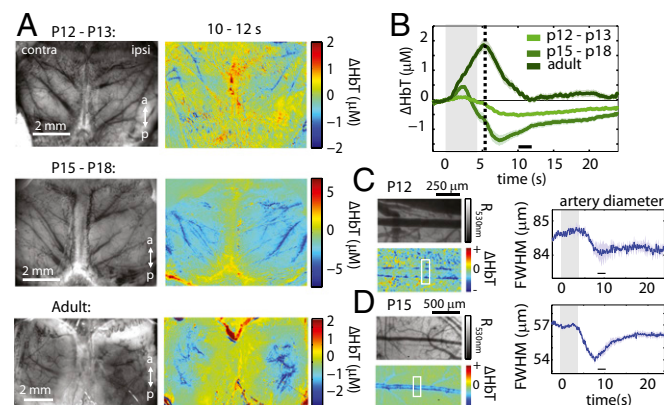
Focusing first on the delayed decrease in HbT, Fig. 3*A* shows bilateral difference images comparing cortical HbT 10–12 s after stimulus onset to baseline in a P13 rat. Decreases in HbT are largely localized to pial arteries projecting toward the midline, suggesting active arterial constriction. Experiments were repeated with the skull and dura overlying the somatosensory cortex removed to allow direct visualization of the vasculature. Time-courses of arterial diameters (full width half-maximum; Fig. 3*C*) confirm that arteries decrease in diameter in response to stimulation, consistent with vasoconstriction.

Although arterial constriction suggests an active process, it is surprising that this component of the neonatal inverted response is bilateral without discernible functional localization. However, examining difference images for the same time-period for P15–P18 and adult age groups (Fig. 3*A*), we find very similar bilateral patterns of decreasing HbT (also confirmed as arterial constriction at P15 in Fig. 3*D*). In fact, we note the presence of an inflection point of the decrease in HbT in all age groups
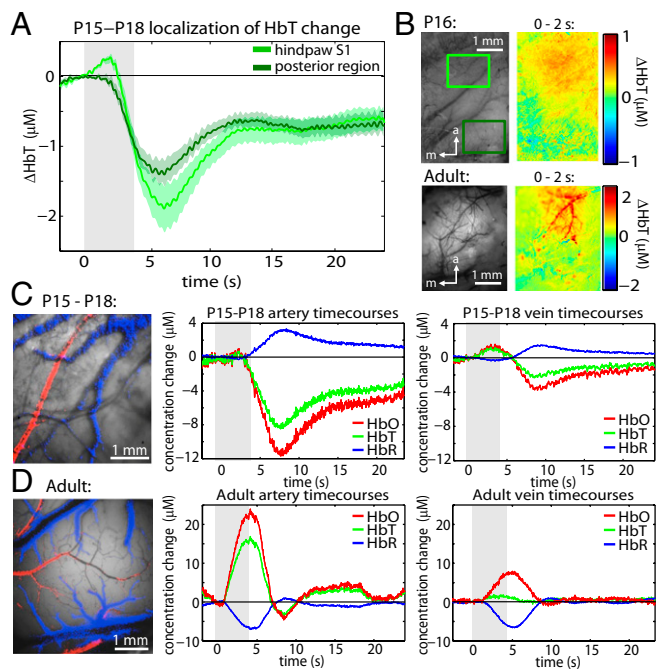
corresponding to the peak time of the adult response (approximated by the dotted line in Fig. 3*B*, also visible in Fig. 2*F*). This "constriction" point is 4.74 ± 1.30 s, 4.56 ± 0.73 s, and 4.74 ± 0.78 s after stimulus onset for each of the increasing age groups, respectively. These similarities across age groups suggest that the mechanism mediating this constriction may be present throughout development, irrespective of the existence of initial hyperemia.

Before vasoconstriction, the P12–P13 response time-course exhibits a small HbR increase and HbO decrease consistent with oxygen consumption. Although localization of this component was difficult to discern, on average, we observed a faster increase in HbR in hindpaw regions (bilaterally) in response to unilateral hindpaw stimulation compared with other regions of the cortex ($P < 0.01$) (Fig. S3). Bilateral ΔHbO, ΔHbR, and ΔHbT image time-sequences for all age groups are included in Figs. S3*F*, S4, and S5.

Development of Positive BOLD. A small, initial phase of stimulus-evoked functional hyperemia becomes apparent by P15–P18. Fig. 4 *A* and *B* show that unlike the constriction phase, this early, positive response is localized to the anterior, hindpaw region of the somatosensory cortex. Fig. S4 shows that this positive response is primarily contralateral, although smaller amplitude ($P < 0.01$), positive ipsilateral responses were observed in some trials. Comparing to the adult response, the adult ΔHbT difference image in Fig. 4*B* shows strong, rapid pial arterial dilation (23), whereas the P16 difference image is more diffuse, suggesting that hyperemia is occurring predominantly at the capillary or precapillary arteriole level without recruiting pial arteries. To explore this effect further, exposed cortex (skull and dura removed) measurements were performed, allowing changes in HbO, HbR, and HbT in arteries and veins to be resolved. In the P15–P18 age group, only a small HbO and HbT increase was observed in the arteries, and an early increase in oxygenation was more prominent in the veins, consistent with hyperemia primarily occurring downstream of pial arteries. In the adult, initial hyperemia is strongly observed in pial arteries. Spatiotemporal unmixing of these time-courses confirms that each is representative of the

Fig. 3. Constriction phase throughout development. (*A Left*) Grayscale (530 nm reflectance) images of the surface vasculature for a representative rat from each group. (*A Right*) ΔHbT difference images for the same rats comparing 10–12 s after stimulus onset to prestimulus baseline. (*B*) Averaged ΔHbT response time-courses for each of the three age groups (*n* = 13, 9, and 8 rats, runs = 72, 68, and 67 runs, respectively) with a dotted-line at the inflection point of the HbT decrease. (*C and D Left*) Regions of interest over pial arteries in exposed-cortex animals, (*Upper*) 530 nm reflectance (R_{530}nm) and (*Lower*) ΔHbT difference images (8–10 s after stimulus onset baseline) for representative p13 (*C*) and p15 (*D*) rats. Blue bars along artery edges indicate vasoconstriction. (*C and D Right*) Time-courses of the diameters of arterial segments indicated (full width half-maximum), averaged over three and eight runs, respectively. Error bounds show SEM.

Kozberg et al.

www.manaraa.com

Fig. 4. Vascular compartment-specific development of the "initial hyperemic" phase. (A) Averaged ΔHbT time-courses from the hindpaw (anterior) region and adjacent posterior regions (n = 3 rats, runs = 27) highlighting localization of initial hyperemia. Error bounds show SEM. (B) Grayscale image (530 nm reflectance) and ΔHbT difference images (0–2 s average after stimulus onset baseline) from a representative P16 rat (runs = 7) and adult rat (runs = 1). (C and D Left) Representative exposed-cortex grayscale images overlaid with pixels spatiotemporally unmixed as arterial (red) and venous (blue) based on their time-courses (Methods). (C and D Right) Time-courses corresponding to pial artery and pial vein changes in HbO, HbR, and HbT for P15–P18 (n = 2 rats, runs = 13) and adult (n = 2 rat, runs = 6) rats, respectively.

behavior of each vascular compartment (Fig. 4 C and D; see Methods and ref. 28). These results suggest that recruitment of pial arteries may be a developmental process that facilitates amplification of initial hyperemia with increasing age.

Discussion

Systemic Blood Pressure Effects. At higher stimulus amplitudes, P12–P13 neonates (developmentally equivalent to human newborns) were found to be highly susceptible to systemic blood pressure increases. The timing and magnitude of these increases closely matched concurrent, adult-like positive cortical "hemodynamic responses," consistent with decreased autoregulation in the neonatal brain (29, 30). This combination of sensitivity to stimulation and underdeveloped autoregulation suggests that fMRI data acquired in neonates and infants may be widely influenced by blood pressure and autoregulation confounds that could be interpreted as differences in the amplitude, sign, and spatial extent of neural activity, even in the absence of true neuronal changes.

Based on these results, we hypothesize that the expectation of a positive BOLD response, and difficulties in selecting and normalizing stimulus amplitudes in nonverbal subjects without systemic blood pressure monitoring, may have led to the use of excessive stimulus amplitudes in some prior neonate studies, resulting in anomalously adult-like positive responses. For example, Colonnese et al.'s fMRI study of neonatal rats obtained positive responses in P13–P15 rats with stimulus amplitudes of 2.12 ± 0.98 mA (1-ms pulse width) and only low levels of isoflurane anesthesia (0.75%), both factors which could have contributed to a systemic blood pressure increase (9).

In our studies, we also observed a decrease in systemic blood pressure in response to lower stimulus amplitudes in both

neonates and adults, possibly due to suppression of catecholamine release (25–27). Accompanied by immature autoregulation, these blood pressure decreases could feasibly produce a passive, bilateral decrease in cortical blood flow or HbT in neonates. We cannot ascribe the arterial constrictions that we observed to this effect, because constrictions begin after the systemic blood pressure decrease begins (Fig. 1D) and appear to be consistent across age groups irrespective of developing autoregulation. However, an early blood pressure drop could produce a small cerebral blood flow decrease (feasibly with no measurable HbT change), which could manifest as a global HbR increase and HbO decrease in the absence of absolute changes in oxygen consumption. This possibility is discussed further below.

Consequences for Interpretation of Functional Imaging Studies.
Interpreting negative BOLD in the neonate. Based on our results, a true neonatal fMRI response would appear as a prolonged period of negative BOLD, the later components of which should be dominated by a ubiquitous "arterial constriction phase." HbR increases before arterial constriction imply an increase in oxygen consumption; however, spatiotemporally differentiating this phase is challenging. Only by analyzing the initial rates of HbR increases did we resolve some diffuse, bilateral localization of oxygen consumption to the hindpaw regions of the somatosensory cortex (Fig. S3). We see three possible explanations for this poor localization: (i) Hindpaw receptive fields may be insufficiently developed to generate a unilaterally localized, synchronized neuronal response. Seelke et al.'s recent electrophysiology study reported that although hindpaw representations are present by P10 in S1, clear topographic organization does not occur until P15, and adult-like body maps only begin to appear by P20 (31). Few studies have addressed whether neonatal somatosensory receptive fields are initially unilateral, and postnatal plasticity might suggest that fields are refined from early bilateral representations (32). (ii) Pure oxygen consumption could have a different spatial distribution compared with the anticipated BOLD signal owing to the use of oxygen by both excitatory and inhibitory neurons, and support cells such as astrocytes. We note that bilateral glucose consumption during unilateral stimulation has been observed in prior adult studies (33, 34). (iii) The effects of blood pressure confounds combined with the large, active constriction phase may overwhelm any small differences in oxygen consumption caused by neuronal activation.

Irrespective of the reason for poor localization, it is clear that negative BOLD signals in the neonatal brain cannot be interpreted in the same way as adult BOLD responses (which are often modeled as positive "hemodynamic response functions" convolved with neuronal input functions) (35). McCandlish et al. showed that the hindpaw region is responsive to peripheral stimulation by P2, and that these responses display similar local field potential waveforms to adults by P4–P5 that are localized to layer IV of the somatosensory cortex (36). This result suggests relatively mature neuronal signaling in the P12–P13 age group and, therefore, points to neurovascular coupling itself being modified or mostly absent during early brain development.
Interpretation of the evolving response. Between P15 and P23, we found that the amplitude of initial hyperemia in the activated region progressively increased, with the response becoming entirely positive by P23 (Fig. 2F). Thus, we would expect that in intermediate age groups a biphasic positive-to-negative fMRI BOLD response would be observed, with the early positive component gradually increasing in amplitude with age. The positive BOLD signal could be expected to localize to responding capillary beds in younger subjects, whereas the negative component is likely to exhibit poor localization. Although maturing spatiotemporal neuronal input functions are likely to influence this evolution, we hypothesize that these features primarily represent the gradual development of mature vasculature and neurovascular signaling. It

Kozberg et al.

www.manaraa.com

NEUROSCIENCE

is therefore important to consider that changes in the amplitude, timing, and localization of positive BOLD signals, even without blood pressure confounds, could reflect maturation of neurovascular coupling as much as the development of neuronal function and connectivity. Equally, studying features of the evolving hemodynamic response could potentially provide new biomarkers for normal or impaired development.

Methodological considerations. Given the prominence of several "global" or spatially diffuse cortical hemodynamic modulations during neonatal development, it should be noted that standard fMRI analysis methods such as global regression could dramatically influence apparent spatial and temporal representations of responses in neonates (37). When comparing responses, it should also be noted that MS-OISI measurements are weighted to superficial layers of the cortex, and both HbT and HbR dynamics were examined in this study. fMRI representations of these results will only reflect HbR dynamics and will depend on the spatial sensitivity of fMRI measurements to changes in the different vascular compartments and cortical layers (Fig. 4C and Figs. S3–S5).

Implications for Brain Development. *Mechanisms of increasing initial hyperemia.* The development of the adult hemodynamic response shows the brain establishing a system that overcompensates for oxygen consumption with local hyperoxygenation. During postnatal development, in addition to neurogenesis and synaptic pruning, many changes occur in the vascular and cellular architecture of the brain that could play a role in the maturation of neurovascular coupling. For example, astrocytes do not mature in rats until approximately P21 and do not reach adult density levels in the cortex until P50 (38, 39). Prostanoids are not synthesized at adult levels until P21 in the rat brain (40), and the vasculature itself is also still undergoing substantial angiogenesis and vascular pruning/remodeling postnatally (41). Cortical vasculature may only begin to take on defined arterial and venous characteristics at around P10 (42), and intravascular upstream signaling mechanisms are not well established in the newborn brain (43, 44). All of these components could therefore be critical to generating reactive cortical hyperemia, and direct comparison between their development and the characteristics of early hyperemia (such as the progression from capillary-level hyperemia to recruitment of pial arteries) could potentially clarify the roles of different cell types in adult neurovascular coupling.

Arterial constriction. In all age groups, irrespective of the level of initial hyperemia, we found consistent evidence that an active, global constriction of pial arterioles occurs 4–5 s after stimulus onset. This result is consistent with previous human infant studies reporting negative BOLD accompanied by blood flow decreases measured using arterial water spin labeling (7) and decreases in HbT observed using NIRS (15). Delayed constriction appears to be driven by a mechanism independent of initial hyperemia and arterial dilation, is present even in the immature brain, and does not change significantly with development. We hypothesize that in adults, this global constriction serves to return elevated HbT levels to baseline, and can accordingly cause HbT to dip below baseline outside of the responding region, potentially underpinning reported "negative surround" responses (33, 45). We hypothesize that this component could be driven via innervation of major vessels from brain regions such as the superior cervical, sphenopalatine and trigeminal ganglia, the locus coeruleus, the raphe nuclei, or nucleus basalis (46, 47, 48).

Oxygen consumption. Prior studies of neonatal functional hemodynamics have suggested that negative BOLD responses could be the result of greater local oxygen demand in neonates than in adults (7, 8, 12, 49). However, although increased oxygen consumption may contribute to neonatal negative BOLD, the lack of responsive hyperemia, and presence of global vasoconstriction that we observe, will inevitably lead to negative BOLD.

Consistent with observations of lower baseline cerebral metabolic rate of oxygen consumption in early neonates compared with adults (50, 51), we conclude then that the presence of negative BOLD does not inherently suggest that oxygen consumption is elevated in the neonatal brain. In fact, decreased baseline consumption may mean higher levels of oxygen availability, providing a potential explanation for how the neonatal brain is able to withstand an early lack of functional hyperemia and the presence of reactive vasoconstrictions. This possibility is also consistent with the ability of the perinatal brain to tolerate low oxygen levels in utero and in preparation for the trauma of delivery (52).

Summary. Overall, the results of this study support earlier findings of negative BOLD responses in neonates and delineate the progression from this inverted response through a biphasic positive-negative period to a fully positive adult response. Our data suggest that there are at least two vascular mechanisms at work in normal neurovascular coupling: (*i*) a global, delayed constriction process, present from early development and (*ii*) a localized initial hyperemia that develops gradually and is not in place at birth. We also observed that stimulus-evoked systemic blood pressure increases can cause apparent adult-like positive BOLD cortical responses in neonates consistent with immature autoregulation. We conclude that the parallel development and complex interplay of autoregulation, neurovascular coupling, and neuronal function in the developing brain should be carefully considered when interpreting hemodynamic measures such as fMRI BOLD in infants and children.

Although further studies are necessary to delineate the cellular and molecular underpinnings of the hemodynamic signatures identified in this work, these results could significantly improve the potential for fMRI to be used for the diagnosis, treatment, and management of neurological, cerebrovascular, and developmental conditions in infants, children, and adults.

Methods

Animal Preparation. Sprague–Dawley rat pups and adults were anesthetized with 1.5 mg/g urethane administered IP before surgery. Glycopyrrolate (0.5 mg/kg) was also administered IP. A rodent pulse oximeter (Kent Scientific MouseSTAT) was used to continuously monitor heart rate and arterial oxygen saturation throughout both surgery and imaging. Core body temperature was maintained at 37 °C by a homeothermic heating system (Stoelting). In some experiments, a femoral arterial cannula was placed to continuously monitor systemic blood pressure (BP-1; World Precision Instruments). Each rat was placed in a customized stereotactic frame, and the skull overlying the left and/or right somatosensory cortices was thinned to translucency by using a dental burr. In some experiments, the skull and dura overlying the somatosensory cortices were removed, and then the cortex was covered with a drop of agarose in artificial CSF and a glass coverslip, and sealed in place using dental acrylic (Henry Schein). Electrodes were inserted into the hindpaws and were connected to a stimulus isolation unit (A360; World Precision Instruments). Stimuli consisted of 3-ms pulses delivered to the hindpaw at 3 Hz for 4 s. Stimuli were 1 mA or less throughout the study, unless otherwise noted. A "run" consisted of five averaged sequential stimulation periods, each with 6 s of prestimulation, 4 s of stimulus, and 20 s of poststimulation. All animal procedures were reviewed and approved by the Columbia University Institutional Animal Care and Use Committee.

Multispectral Optical Intrinsic Spectral Imaging. Imaging was performed using a custom MS-OISI system composed of a Dalsa 1M60 CCD camera, configured to acquire images synchronously with strobing blue, green, and red light emitting diodes (LEDs, 470, 530, and 625 nm, respectively: M470L2, M530L2, and M625L2; Thorlabs) (22). Green and blue LEDs were filtered by using FB530-10 (Thorlabs) or 6701 (Edmund Optics) and FB460-60 (Thorlabs) filters, respectively. The triwavelength data were collected at 75 frames per second (fps), which is equivalent to 25 fps per wavelength, with a 5-ms exposure time and 512 × 512 pixel resolution.

Data Processing. All imaging data were low-pass filtered at 3 Hz, divided by its prestimulus baseline, and then converted to ΔHbO and ΔHbR by using the

Kozberg et al.

www.manaraa.com

modified Beer–Lambert law with wavelength-dependent path-length factors derived from Monte Carlo modeling (22, 53, 54). Because we acquire three-wavelength data, but have only two unknowns, ΔHbO and ΔHbR were calculated with all three possible pairs of wavelengths to confirm proper conversions. Parameter averages in Fig. 2 *D* and *E* were calculated by first averaging all runs within each rat and then averaging these single rat averages within each age group. A Student *t* test was used for parameter comparisons. Spatiotemporal unmixing in Fig. 4 *C* and *D* was performed as described in Hillman et al. (28): Concatenated HbO, HbR, and HbT time-courses were extracted from representative regions corresponding to arteries, parenchyma, and veins within the responding hindpaw region. Least squares nonnegative linear unmixing was then performed to quantify the occurrence of each time-course in each pixel within the image time-series. If these pixels lined up well to each of the selected vascular compartments, time-courses were considered representative of their respective vascular compartments.

1. Attwell D, Iadecola C (2002) The neural basis of functional brain imaging signals. *Trends Neurosci* 25(12):621–625.
2. Sirotin YB, Hillman EMC, Bordier C, Das A (2009) Spatiotemporal precision and hemodynamic mechanism of optical point spreads in alert primates. *Proc Natl Acad Sci USA* 106(43):18390–18395.
3. Heeger DJ, Ress D (2002) What does fMRI tell us about neuronal activity? *Nat Rev Neurosci* 3(2):142–151.
4. Meek JH, et al. (1998) Regional haemodynamic responses to visual stimulation in awake infants. *Pediatr Res* 43(6):840–843.
5. Taga G, Asakawa K, Maki A, Konishi Y, Koizumi H (2003) Brain imaging in awake infants by near-infrared optical topography. *Proc Natl Acad Sci USA* 100(19):10722–10727.
6. Harris JJ, Reynell C, Attwell D (2011) The physiology of developmental changes in BOLD functional imaging signals. *Dev Cogn Neurosci* 1(3):199–216.
7. Born AP, Rostrup E, Miranda MJ, Larsson HBW, Lou HC (2002) Visual cortex reactivity in sedated children examined with perfusion MRI (FAIR). *Magn Reson Imaging* 20(2):199–205.
8. Yamada H, et al. (1997) A rapid brain metabolic change in infants detected by fMRI. *Neuroreport* 8(17):3775–3778.
9. Colonnese MT, Phillips MA, Constantine-Paton M, Kaila K, Jasanoff A (2008) Development of hemodynamic responses and functional connectivity in rat somatosensory cortex. *Nat Neurosci* 11(1):72–79.
10. Arichi T, et al. (2010) Somatosensory cortical activation identified by functional MRI in preterm and term infants. *Neuroimage* 49(3):2063–2071.
11. Liao SM, et al. (2010) Neonatal hemodynamic response to visual cortex activity: High-density near-infrared spectroscopy study. *J Biomed Opt* 15(2):026010.
12. Yamada H, et al. (2000) A milestone for normal development of the infantile brain detected by functional MRI. *Neurology* 55(2):218–223.
13. Born AP, et al. (2000) Functional magnetic resonance imaging of the normal and abnormal visual system in early life. *Neuropediatrics* 31(1):24–32.
14. Martin E (1999) Visual processing in infants and children studied using functional MRI. *Pediatr Res* 46(2):135–140.
15. Kusaka T, et al. (2004) Noninvasive optical imaging in the visual cortex in young infants. *Hum Brain Mapp* 22(2):122–132.
16. Rombouts SA, Valk IJ, Hart AA, Scheltens P, van der Knaap MS; Sie LTL (2001) Functional MRI of visual cortex in sedated 18 month-old infants with or without periventricular leukomalacia. *Dev Med Child Neurol* 43(7):486–490.
17. Muramoto S, et al. (2002) Age-dependent change in metabolic response to photic stimulation of the primary visual cortex in infants: Functional magnetic resonance imaging study. *J Comput Assist Tomogr* 26(6):894–901.
18. Anderson AW, et al. (2001) Neonatal auditory activation detected by functional magnetic resonance imaging. *Magn Reson Imaging* 19(1):1–5.
19. Born P, et al. (1998) Visual activation in infants and young children studied by functional magnetic resonance imaging. *Pediatr Res* 44(4):578–583.
20. Ment LR, Constable RT (2007) Injury and recovery in the developing brain: Evidence from functional MRI studies of prematurely born children. *Nat Clin Pract Neurol* 3(10):558–571.
21. Quinn R (2005) Comparing rat's to human's age: How old is my rat in people years? *Nutrition* 21(6):775–777.
22. Bouchard MB, Chen BR, Burgess SA, Hillman EMC (2009) Ultra-fast multispectral optical imaging of cortical oxygenation and blood flow dynamics. *Opt Express* 17(18):15670–15678.
23. Chen BR, Bouchard MB, McCaslin AFH, Burgess SA, Hillman EMC (2011) High-speed vascular dynamics of the hemodynamic response. *Neuroimage* 54(2):1021–1030.
24. Kennerley AJ, et al. (2005) Concurrent fMRI and optical measures for the investigation of the hemodynamic response function. *Magn Reson Med* 54(2):354–365.
25. Sato A (1987) Neural mechanisms of somatic sensory regulation of catecholamine secretion from the adrenal gland. *Adv Biophys* 23:39–80.
26. Suzuki ASM, Shimura M (2010) Changes in blood pressure induced by electrical stimulation of the femur in anesthetized rats. *Auton Neurosci* 158(1-2):39–43.
27. Kurosawa M (1985) [Effects of noxious and innocuous cutaneous stimulation on adrenal sympathetic efferent nerve activity in rats]. *Hokkaido Igaku Zasshi* 60(4):509–527.
28. Hillman EMC, et al. (2007) Depth-resolved optical imaging and microscopy of vascular compartment dynamics during somatosensory stimulation. *Neuroimage* 35(1):89–104.
29. Brady KM, et al. (2010) Monitoring cerebral blood flow pressure autoregulation in pediatric patients during cardiac surgery. *Stroke* 41(9):1957–1962.
30. Greisen G (2009) To autoregulate or not to autoregulate—that is no longer the question. *Semin Pediatr Neurol* 16(4):207–215.
31. Seelke AMH, Dooley JC, Krubitzer LA (2012) The emergence of somatotopic maps of the body in S1 in rats: The correspondence between functional and anatomical organization. *PLoS ONE* 7(2):e32322.
32. Leonard CT, Goldberger ME (1987) Consequences of damage to the sensorimotor cortex in neonatal and adult cats. II. Maintenance of exuberant projections. *Brain Res* 429(1):15–30.
33. Devor A, et al. (2008) Stimulus-induced changes in blood flow and 2-deoxyglucose uptake dissociate in ipsilateral somatosensory cortex. *J Neurosci* 28(53):14347–14357.
34. Weber B, Fouad K, Burger C, Buck A (2002) White matter glucose metabolism during intracortical electrostimulation: A quantitative [(18)F]Fluorodeoxyglucose autoradiography study in the rat. *Neuroimage* 16(4):993–998.
35. Cardoso MM, Sirotin YB, Lima B, Glushenkova E, Das A (2012) The neuroimaging signal is a linear sum of neurally distinct stimulus- and task-related components. *Nat Neurosci* 15(9):1298–1306.
36. McCandlish CA, Li CX, Waters RS (1993) Early development of the SI cortical barrel field representation in neonatal rats follows a lateral-to-medial gradient: An electrophysiological study. *Exp Brain Res* 92(3):369–374.
37. Monti MM (2011) Statistical analysis of fMRI time-series: A critical review of the GLM approach. *Front Hum Neurosci* 5:28.
38. Müller CM (1992) Astrocytes in cat visual cortex studied by GFAP and S-100 immunocytochemistry during postnatal development. *J Comp Neurol* 317(3):309–323.
39. Stichel CC, Müller CM, Zilles K (1991) Distribution of glial fibrillary acidic protein and vimentin immunoreactivity during rat visual cortex development. *J Neurocytol* 20(2):97–108.
40. Seregi A, Keller M, Hertting G (1987) Are cerebral prostanoids of astroglial origin? Studies on the prostanoid forming system in developing rat brain and primary cultures of rat astrocytes. *Brain Res* 404(1-2):113–120.
41. Norman MG, O'Kusky JR (1986) The growth and development of microvasculature in human cerebral cortex. *J Neuropathol Exp Neurol* 45(3):222–232.
42. Rowan RA, Maxwell DS (1981) Patterns of vascular sprouting in the postnatal development of the cerebral cortex of the rat. *Am J Anat* 160(3):247–255.
43. Errede M, et al. (2002) Differential expression of connexin43 in foetal, adult and tumour-associated human brain endothelial cells. *Histochem J* 34(6-7):265–271.
44. Fujimoto K (1995) Pericyte-endothelial gap junctions in developing rat cerebral capillaries: A fine structural study. *Anat Rec* 242(4):562–565.
45. Boas DA, Jones SR, Devor A, Huppert TJ, Dale AM (2008) A vascular anatomical network model of the spatio-temporal response to brain activation. *Neuroimage* 40(3):1116–1129.
46. Girouard H, Iadecola C (2006) Neurovascular coupling in the normal brain and in hypertension, stroke, and Alzheimer disease. *J Appl Physiol* 100(1):328–335.
47. Iadecola C (2004) Neurovascular regulation in the normal brain and in Alzheimer's disease. *Nat Rev Neurosci* 5(5):347–360.
48. Bekar LK, Wei HS, Nedergaard M (2012) The locus coeruleus-norepinephrine network optimizes coupling of cerebral blood volume with oxygen demand. *J Cereb Blood Flow Metab* 32(12):2135–2145.
49. Huttenlocher PR, de Courten C, Garey LJ, Van der Loos H (1982) Synaptogenesis in human visual cortex—evidence for synapse elimination during normal development. *Neurosci Lett* 33(3):247–252.
50. Altman DI, Perlman JM, Volpe JJ, Powers WJ (1993) Cerebral oxygen metabolism in newborns. *Pediatrics* 92(1):99–104.
51. Takahashi T, Shirane R, Sato S, Yoshimoto T (1999) Developmental changes of cerebral blood flow and oxygen metabolism in children. *AJNR Am J Neuroradiol* 20(5):917–922.
52. Singer D (1999) Neonatal tolerance to hypoxia: A comparative-physiological approach. *Comp Biochem Physiol A: Mol Integr Physiol* 123(3):221–234.
53. Hillman EMC (2007) Optical brain imaging in vivo: Techniques and applications from animal to man. *J Biomed Opt* 12(5):051402.
54. Sakaguchi K, et al. (2007) Experimental prediction of the wavelength-dependent path-length factor for optical intrinsic signal analysis. *Appl Opt* 46(14):2769–2777.

NEUROSCIENCE

Kozberg et al.